Mining of Mineral Deposits
Volume 19 (2025), Issue 4, 12-21

MMD JOURNAL / MINING.IN.UA

https://doi.org/10.33271/mining19.04.012

Geochemical distribution and correlations of Cd-Ag-Sb in relation to Pb-Zn mineralization at the Trepça mine, Kosovo

Festim Kutllovci [1], Berat Sinani [1*]

[1] *University "Isa Boletini", Mitrovica, Kosovo*

**Corresponding author: e-mail berat.sinani@umib.net*

Abstract

Purpose. The study aims to investigate the geochemical distribution and inter-element correlations of cadmium (Cd), silver (Ag), and antimony (Sb) within the polymetallic Pb-Zn ore system of the Trepça mine (Kosovo). These elements, considered technologically critical due to their growing industrial relevance, were examined to define their paragenetic relationships with the principal sulfide minerals (galena and sphalerite), and to elucidate their spatial patterns within the mineralized zones.

Methods. Representative samples were collected from each active ore body within Horizons VIII-XI of the Trepça deposit. Each sample underwent drying, multi-stage grinding, acid digestion, and chemical analysis by inductively coupled plasma mass spectrometry (ICP-MS). The obtained analytical data were statistically processed to determine descriptive parameters and Pearson correlation coefficients, while geochemical contour maps were generated using Surfer software to visualize spatial distributions.

Findings. Cadmium concentrations ranged from 34 to 1125 ppm (average ≈ 308 ppm), silver from 20 to 389 ppm (average ≈ 93 ppm), and antimony from 42 to 512 ppm (average ≈ 171 ppm). Strong positive correlations were observed between Ag and Pb ($r = 0.94$) and between Cd and Zn ($r = 0.77$), indicating two dominant geochemical associations: a Pb-Ag paragenetic group and a Zn-Cd-Sb assemblage. The vertical and spatial distributions confirm a continuous Pb-Zn-Ag-Cd-Sb zonation typical of hydrothermal replacement systems.

Originality. This work provides the first integrated statistical and spatial characterization of Ag-Cd-Sb in relation to Pb-Zn mineralization in the Trepça mine. It demonstrates the vertical persistence of these geochemical patterns across multiple horizons and highlights the evolving hydrothermal conditions controlling their deposition.

Practical implications. The identified Pb-Ag and Zn-Cd-Sb assemblages serve as reliable geochemical indicators for exploration and selective ore processing. The results confirm the potential recovery of Ag, Cd, and Sb as valuable by-products from Pb-Zn ores, contributing to more sustainable and resource-efficient utilization of the Trepça deposit.

Keywords: *Trepça, mine, geochemistry, distribution, critical minerals*

1. Introduction

The history of silver, lead, and zinc mining in Kosovo is closely intertwined with the broader industrial and economic development of the region. In the modern era, the name Trepça has become synonymous with the production of these metals and with the evolution of mining in Kosovo [1], [2]. The Trepça complex represents one of the most significant polymetallic mining areas in Southeastern Europe, hosting numerous Pb-Zn occurrences and substantial ore reserves that have played a decisive role in the country's economic growth. The exploitation of lead and zinc ores in this region dates back to the Roman period, whereas systematic geological investigations began in 1926 under British management and continued through the 1930s, marking the onset of modern mining operations. In 1941, Trepça came under German control and remained so until the end of World War II [3], [4].

The polymetallic deposits of Trepça extend across much of Kosovo, particularly along the Vardar zone [5]. The lead and zinc reserves are concentrated mainly within active mining areas and nearby deposits. Historically, Trepça functioned as an integrated mining and metallurgical system and was once considered among the largest European producers of non-ferrous (Pb, Zn, Bi), rare (Cd, Ge), and precious (Ag, Au) metals. In addition to Pb-Zn concentrates, copper was also successfully processed, together with minor but economically important elements such as germanium, selenium, and tellurium [6], [7].

In recent decades, technological advances and the rising global demand for critical raw materials (CRMs) have renewed interest in the different ore system [8], [9]. Beyond its traditional Pb-Zn-Ag mineralization, the deposit contains measurable concentrations of cadmium (Cd) and antimony (Sb) elements of increasing industrial and strategic importance. Given the geological complexity of Trepça and its polymetallic nature, studying the distribution of these critical elements provides valuable insights into both ore-forming processes and potential economic recovery [10].

Accordingly, the present study focuses on the geochemical distribution and correlation of Ag, Cd, and Sb within the

Received: 23 April 2025. Accepted: 22 October 2025. Available online: 30 December 2025

Mining of Mineral Deposits. ISSN 2415-3443 (Online) | ISSN 2415-3435 (Print)

Trepça mine, specifically in Horizons VIII-XI, which represent the active mineralized zones of the deposit. The research aims to identify paragenetic relationships among these critical elements and the major Pb-Zn sulfide minerals (galena and sphalerite), to better understand their spatial and vertical zonation patterns. The general geological framework of the study area, including the locations of active mines within Kosovo, is illustrated in Figure 1, with particular emphasis on the Trepça mining district.

Figure 1. Mineral map of Kosovo [11]

From Figure 1, it can be observed that the territory of Kosovo is geologically diverse and highly mineralized, reflecting a complex tectono-metallogenic history. This geological complexity, combined with the increasing global demand for critical raw materials (CRMs), highlights the need for new research focused on the utilization of these resources and the reassessment of mineral deposits that have been exploited for decades mainly for major metals such as Pb, Zn, Cr, and Mg.

During the last two decades, technological progress and the transition toward sustainable and high-technology industries have intensified the demand for critical elements such as Cd, Ag, and Sb. The selection of these elements in the present study is based on their notably high concentrations within hydrothermal sources of the Trepça mine, where they occur in close association with Pb-Zn sulfide mineralization.

The geochemical investigation of Cd, Ag, and Sb, as well as their spatial distribution and correlation with Pb-Zn ores, is therefore of fundamental importance for understanding their sources, genetic relationships, and distribution patterns within the deposit. The Trepça mining complex and its surrounding resources, as illustrated in Figure 2, have long been of strategic importance not only for traditional Pb-Zn production, but also for the identification, evaluation, and potential recovery of critical elements that today possess growing economic significance in countries rich in such mineral resources.

Every three years, the European Union updates its List of Critical Raw Materials (CRMs), which identifies raw materials of high economic importance and high supply risk. Since its first publication in 2011, the list has been periodically revised to reflect technological progress, market changes, and global supply dynamics [12], [13]. The current list includes 35 raw materials of critical and strategic relevance (Table 1), encompassing elements essential for the development of advanced technologies, renewable energy systems, and the green transition.

Table 1. List of critical raw materials year by year [14], [15]

Elements	2011	2014	2017	2020	2023
Number of TCE elements	14	20	27	35	34
Antimony	✓	✓	✓	✓	✓
Arsenic					✓
Barite			✓	✓	✓
Bauxite (Aluminium)				✓	✓
Beryllium	✓	✓	✓	✓	✓
Bismuth			✓	✓	✓
Borate		✓	✓	✓	✓
Cadmium	✓	✓	✓	✓	
Chromium		✓			
Cobalt					✓
Coking Coal	✓	✓	✓	✓	✓
Copper					✓
Feldspar					✓
Fluorspar	✓	✓	✓	✓	✓
Gallium	✓	✓	✓	✓	✓
Germanium	✓	✓	✓	✓	✓
Hafnium			✓		✓
Helium			✓	✓	✓
Heavy REEs	✓	✓	✓	✓	✓
Indium	✓	✓	✓	✓	
Light REEs	✓	✓	✓	✓	✓
Lithium				✓	✓
Magnesite		✓			
Magnesium	✓	✓	✓	✓	✓
Manganese					✓
Natural Graphite	✓	✓	✓	✓	✓
Natural Rubber			✓	✓	
Nickel					✓
Niobium	✓	✓	✓	✓	✓
Phosphate Rock		✓	✓	✓	✓
Platinum group metals	✓	✓	✓	✓	✓
Phosphorus			✓	✓	✓
Scandium			✓	✓	✓
Silicon Metal		✓	✓	✓	✓
Strontium				✓	✓
Tantalum	✓		✓	✓	✓
Titanium Metal				✓	✓
Tungsten	✓	✓	✓	✓	✓
Vanadium			✓	✓	✓

Note: TCE – Technology-Critical Elements included in the EU List of Critical Raw Materials for each reference year

The increasing demand for CRMs is directly linked to the ongoing transformation toward a low-carbon and resource-efficient economy. Critical materials such as antimony, cadmium, cobalt, lithium, and rare earth elements play a vital role in renewable energy production, electric mobility, and digitalization. Consequently, ensuring a secure and sustainable supply of these materials has become a strategic priority for the European Union. To achieve this, the European Commission has encouraged new exploration and reassessment of historical mining districts across member states, aiming to identify untapped or secondary sources of CRMs and reduce dependence on geopolitically unstable suppliers.

Among the investigated elements, antimony (Sb) is classified by the European Union (2023) as a critical raw material due to its strategic importance and supply risk. Silver (Ag) and cadmium (Cd), while technologically important in metallurgical and energy applications, are not included in the EU 2023 critical list. Given their paragenetic association with Pb-Zn mineralization at Trepça, their distribution nonetheless has clear geological and economic relevance [16], [17].

Antimony (Sb) is primarily utilized as a flame retardant in polymers, coatings, and textiles, and it also serves in the production of diodes and antimonial lead alloys key components of secondary lead smelters [18]. Developed economies such as the European Union and the United States have officially recognized antimony as a critical raw material [19]. Therefore, understanding their distribution in mineralized systems such as Trepça provides not only geological but also economic insights into the potential of critical element recovery from polymetallic deposits.

2. Geological characteristics of study area

The Trepça geological complex comprises several resource zones, including the Trepça-Stantërg region, the Kishnica-Novo Brdo region, and the Kopaonik mines region. The main ore reserves are concentrated in areas near Belo Brdo and Crnac [6]. Figure 2 presents a topographic map illustrating the distribution of metallic resources within the Trepça region, which includes the following deposits: Stantërg, Melenica, Maxhera, Mazhiq-Maja Madhe, Gjidomë-Mazhiq, Rashan, Tërstenë, and Zijaqë.

Figure 2. Topographic map of the Trepça region

All of these deposits are integral parts of the Trepça complex, as illustrated in Figure 2, which presents the topographic map of the Trepça region. From Figure 2, it can be observed that within a relatively small area there is a notably dense distribution of mineralization. Figure 3 provides the geological structure of the study area, represented by the geological formations encompassing the broader study region. This area also includes the Pb–Zn mineral resources distributed throughout the wider Trepça zone.

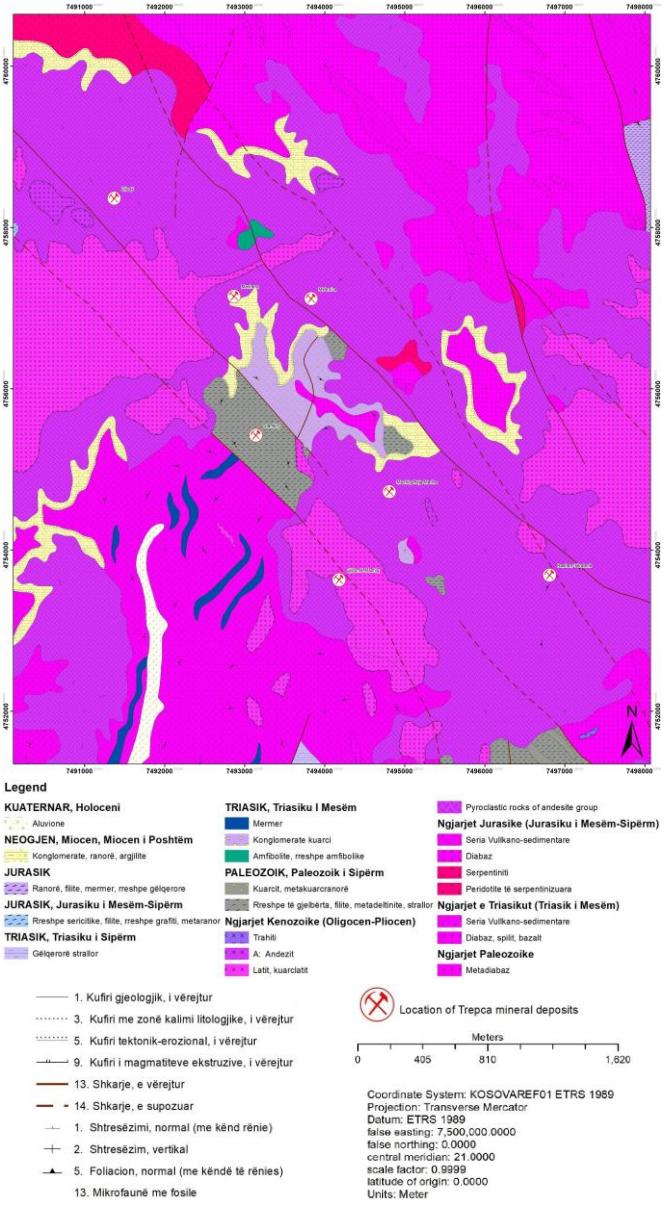

Figure 3. Geological map of the Trepça region [20]

From the figure presented, it can be observed that the geological formations of the Trepça mine and its surrounding study area are characterized by a complex lithological and structural composition. The region comprises diverse stratigraphic units ranging from the Paleozoic to the Quaternary, including volcanic, sedimentary, and metamorphic sequences. Numerous tectonic and fault lines intersect the area, indicating intensive geological activity and deformation processes that have significantly influenced the localization and distribution of Pb-Zn and associated mineral deposits within the Trepça complex.

3. Materials and methods

3.1. Sampling and laboratory procedures

For the realization of this study, standard geological sampling and analytical procedures were applied. Representative samples were collected from each active ore body within Horizons VIII–XI of the Trepça mine. In every ore body, three subsamples were taken to ensure an accurate representation of the mineralization characteristics and to reduce sampling bias. The collected samples were air-dried at 104°C to remove moisture, then subjected to three successive milling stages (primary, secondary, and tertiary grinding) to achieve homogeneous particle size and compositional uniformity. All collected material was carefully logged and labeled according to its spatial position and lithological characteristics to maintain full traceability throughout subsequent analytical stages.

After homogenization, the powdered samples were digested using an acid digestion procedure and analyzed for elemental composition by inductively coupled plasma mass spectrometry (ICP-MS) at the Artmer Institute, Zonguldak University (Türkiye). The analytical accuracy and reproducibility were verified by replicate measurements and certified reference materials. The entire methodological workflow from sampling to statistical evaluation is illustrated in Figure 4.

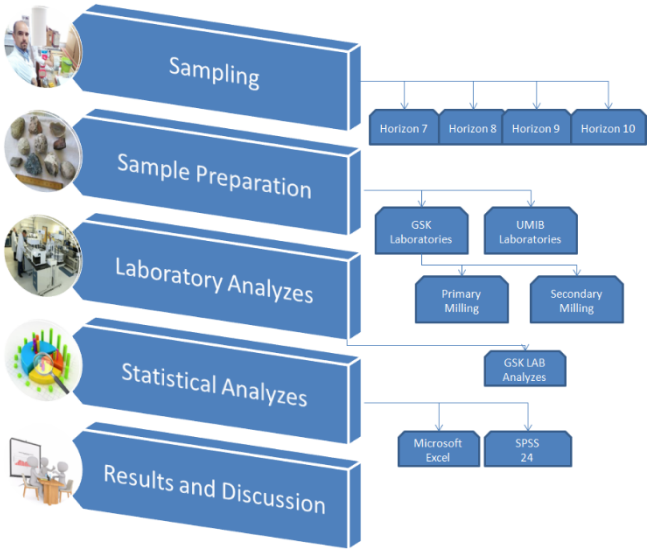

Figure 4. Scheme of implementation of this study

The schematic workflow presented in Figure 4 outlines the overall procedure adopted in this study, from field sampling to sample preparation and laboratory analysis. The process begins with the systematic collection of representative material from the active ore bodies located in Horizons VIII-XI of the Trepça mine. Subsequent preparation included drying at controlled temperature, followed by multi-stage milling to ensure particle-size uniformity and chemical homogeneity. Laboratory analyses were performed on homogenized samples to determine the concentrations of Pb, Zn, Ag, Cd, and Sb using certified analytical procedures.

This structured workflow ensured the traceability of each analytical stage, minimized the influence of sampling and preparation errors, and guaranteed that all data used for further interpretation were obtained under standardized and reproducible conditions.

3.2. Analytical and statistical methods

The obtained ICP-MS data were systematically processed and evaluated using a combination of analytical and statistical software tools to ensure accuracy, consistency, and interpretive reliability [21], [22]. The raw data were first organized and verified in Microsoft Excel, where outlier screening and preliminary statistical checks were performed. The program was also used to compute elemental ratios and generate basic visualizations that facilitated the identification of general trends and anomalies among Pb, Zn, Ag, Cd, and Sb concentrations.

Subsequently, detailed statistical analysis was conducted in SPSS Statistics 24 [23]. Descriptive statistical parameters including mean, median, mode, standard deviation, variance, coefficient of variation, skewness, and kurtosis were calculated for each analyzed element to characterize the variability and distribution of data. Correlation analyses were then performed to determine the strength and direction of inter-element relationships, providing insight into their geochemical associations and potential paragenetic links within the mineralized zones. The use of both descriptive and inferential statistics allowed for a robust quantitative characterization of the dataset, minimizing the influence of random variation and analytical uncertainty [24], [25].

Spatial data analysis and geochemical mapping were performed using Golden Software Surfer 13, applying contour interpolation techniques such as Kriging and Inverse Distance Weighting (IDW) to visualize the distribution patterns of Pb, Zn, Ag, Cd, and Sb across Horizons VIII-XI [26], [27]. The resulting contour maps illustrate both horizontal and vertical zoning of critical elements within the ore bodies, reflecting the underlying geological structure and hydrothermal fluid migration pathways.

By integrating statistical and spatial approaches, the study ensured a comprehensive understanding of the geochemical relationships and mineralogical controls governing the occurrence of these elements. This combined methodology created a unified basis for interpreting paragenetic associations and vertical continuity of mineralization, forming an analytical framework.

3.3. Data validation and quality control

To ensure the reliability and reproducibility of the analytical results, rigorous data validation and quality control procedures were implemented throughout all stages of the study. During the sampling and laboratory preparation phases, strict protocols were followed to prevent cross-contamination and to maintain sample representativeness [28], [29]. All analytical operations were conducted under standardized laboratory conditions using certified reagents and calibrated equipment.

For the ICP-MS analyses, instrument performance was monitored through the use of certified reference materials (CRMs), procedural blanks, and duplicate samples. Analytical precision and accuracy were assessed by comparing measured concentrations with certified values, yielding deviations within ±5%, which confirms the consistency of the applied methodology [30]. Randomly selected samples were reanalyzed to evaluate measurement repeatability, and the obtained results demonstrated high reproducibility for all analyzed elements.

Prior to statistical evaluation, the dataset underwent screening for outliers and missing values. Outliers were examined using boxplots, Z-score thresholds, and the Grubbs test to determine whether extreme values reflected genuine geological variation or analytical artefacts [31], [32]. Data identified as analytical anomalies were excluded from the statistical processing but retained in the metadata for reference. The validated dataset was then normalized and processed for descriptive and correlation analyses, ensuring that subsequent statistical and spatial interpretations were based on accurate and quality-assured data [33].

The applied validation and quality control procedures ensured that all analytical results were both statistically robust and geochemically representative, providing a solid foundation for the interpretation of spatial and vertical distribution patterns discussed in next section.

4. Results and discussion

4.1. Statistical and geochemical characterization of Pb-Zn-Ag-Cd-Sb concentrations

To establish the concentration ranges and geochemical relationships between the analyzed elements, a comprehensive statistical evaluation was carried out based on the results of ICP-MS analyses. The obtained data provide a quantitative insight into the distribution of lead, zinc, silver, cadmium, and antimony within the ore samples collected from Horizons VIII-XI. Obtained results serve as the basis for identifying compositional trends, inter-element associations, and subsequent spatial-geochemical interpretations. The summarized analytical data are presented in Table 2.

Table 2. Results from laboratory analyses

Sample	Concentration of major and critical elements, ppm				
	Pb	Zn	Ag	Cd	Sb
127	15667	11046	20	34	ND
130	122390	98053	113	362	168
138/A	7609	18719	20	44	ND
139/C	155480	64447	153	368	154
136	5348	3398	17	ND	127
139/B0	3845	92661	ND	271	115
139/F1	5357	17284	20	57	291
149/C	26756	375269	35	1125	427
146	2342	51325	ND	182	117
140	2393	60828	ND	230	168
149/C	151071	1862	80	205	64
147/N	28859	30443	28	107	44
149/C3	12130	9458	20	40	56
149/C2	22960	32185	38	115	512
149/F	314359	6571	389	714	415
158/A	251425	31174	168	546	170
154	3877	467	31	ND	ND
156	5826	94352	22	280	504
150	2659	339	22	ND	67

For instance, sample 149/F shows notably high concentrations of Ag and Cd, accompanied by elevated Pb and Zn values, indicating a close geochemical association among these elements. In contrast, Sb displays a more heterogeneous and irregular distribution, suggesting a variable occurrence within different mineral phases. To better quantify these variations and assess the overall geochemical behavior of the analyzed elements, descriptive statistical parameters for each element are presented in Table 3.

Table 3. Descriptive statistics of selected elements

Descriptive statistics	Concentration of elements, ppm				
Statistic	Pb	Zn	Ag	Cd	Sb
Mean	60018.58	52625.32	61.89	246.32	178.89
Median	12130.00	30443.00	22.00	182.00	127.00
Mode	–	–	20.00	0.00	0.00
Standard deviation	93759.52	84869.78	93.28	288.65	168.84
Variance	8790847102.92	7202879799.01	8700.32	83319.56	28505.32
Coefficient of variation	1.56	1.61	1.51	1.17	0.94
Minimum	2342.00	339.00	0.00	0.00	0.00
Maximum	314359.00	375269.00	389.00	1125.00	512.00
Range	312017.00	374930.00	389.00	1125.00	512.00
Interquartile range	71012.00	54623.00	39.00	279.00	170.50
Skewness	1.77	3.34	2.74	1.88	0.98
Kurtosis	2.25	12.72	8.44	3.93	-0.27

Table 3 presents the descriptive statistics for the analyzed elements, reflecting the distribution of their concentrations within the studied ore samples. The results show relatively high mean values of Pb and Zn, confirming their sulfide origin typical of galena and sphalerite mineralization. Silver exhibits an average concentration of 61.89 ppm and a median of 22 ppm, with a standard deviation of 92.28 ppm, indicating significant spatial and geochemical variability. The positive skewness and elevated kurtosis values also suggest an uneven distribution and a strong association between Pb, Zn, and Ag. Cadmium demonstrates a moderately high mean concentration of 246.32 ppm and a median of 182 ppm, reflecting a relatively stable distribution compared with Ag and Sb; this is confirmed by its coefficient of variation (1.17), which indicates moderate variability.

Antimony shows a mean of 178.89 ppm and a median of 127 ppm, with a low coefficient of variation (0.94), implying a homogeneous and uniform distribution of Sb across the examined ore bodies.

To further evaluate the inter-element relationships, Table 4 presents the correlation matrix of the analyzed elements in order to assess their geochemical associations with Pb and Zn.

Table 4. Correlation matrix for selected elements

Elements, ppm	Pb	Zn	Ag	Cd	Sb
Pb	1.00				
Zn	-0.10	1.00			
Ag	0.94	-0.10	1.00		
Cd	0.52	0.77	0.52	1.00	
Sb	0.19	0.44	0.30	0.54	1.00

The correlation analysis presented in Table 4 reveals strong geochemical relationships among the analyzed elements, reflecting common genetic and mineralization mechanisms. A very high positive correlation between Pb and Ag ($r = 0.94$) indicates that the occurrence of Ag is closely linked to Pb sulfide mineralization, particularly galena. Lead also shows a moderate correlation with Cd ($r = 0.52$), suggesting limited but notable incorporation of Cd within Pb-bearing phases. Conversely, Cd exhibits a strong positive correlation with Zn ($r = 0.77$), confirming its preferential association with sphalerite, where Cd commonly substitutes for Zn in the crystal lattice. Zinc and Sb show a moderate correlation ($r = 0.44$), while Cd and Sb display a similar relationship ($r = 0.54$), implying that Sb tends to occur in secondary associations with both Zn- and Cd-bearing sulfide minerals.

In general, the correlation analysis identifies two principal geochemical associations. The first is the Pb-Ag group, which is strongly related to galena mineralization and reflects the paragenetic connection between these elements. The second is the Zn-Cd-Sb group, associated with sphalerite-bearing zones, where Cd and Sb frequently occur as isomorphic substitutions within the mineral lattice. These relationships confirm the presence of two genetically distinct but spatially overlapping mineralization assemblages within the studied ore bodies.

4.2. Spatial distribution and vertical zoning of Pb-Zn-Ag-Cd-Sb mineralization (Horizons VIII-XI)

To evaluate the geochemical relationships among Pb, Zn, Ag, Cd, and Sb, a spatial analysis was carried out for Horizon VIII using contour mapping based on ICP-MS data. This analysis allows to visualize the distribution patterns of critical elements in relation to the main sulfide mineralization and to determine the paragenetic associations among them. Figure 5 presents the spatial distribution maps of the analyzed elements in Horizon VIII, illustrating the geochemical zoning typical of Pb-Zn hydrothermal systems. These contour maps show the concentration fields of Pb-Zn-Ag-Cd-Sb in Horizon VIII of the Trepça mine. The figures were generated using Surfer 13 software based on analytical data obtained by ICP-MS.

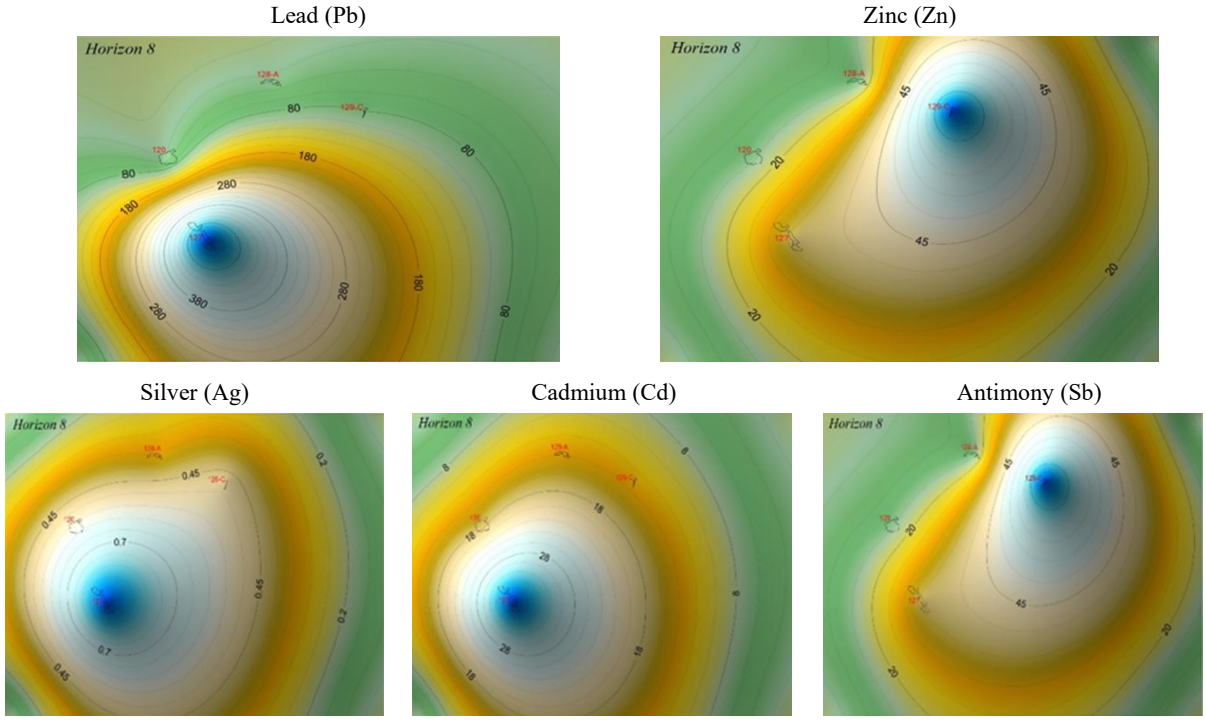

Figure 5. Spatial distribution maps of selected elements in Horizon VIII

The obtained results indicate a distinct zoning pattern within the ore bodies. Lead (Fig. 5a) displays maximum concentrations in the central part of the deposit, forming the core of the mineralization zone dominated by galena (PbS). Zinc (Fig. 5b) exhibits a broader and more uniform distribution, partly overlapping with Pb but extending outward, characteristic of sphalerite (ZnS). Silver (Fig. 5c) closely follows the Pb distribution, confirming a paragenetic relationship between Ag and galena, including its occurrence in Ag-bearing minerals such as tetrahedrite and freibergite. Cadmium (Fig. 5d) is concentrated along the peripheries of Zn-rich zones, reflecting its isomorphic substitution within the sphalerite structure. Antimony (Fig. 5e) shows a relatively homogeneous but intermediate pattern, overlapping both Pb- and Zn-enriched areas, implying its later-stage deposition and association with both mineral phases. Overall, the spatial correlation observed in Horizon VIII confirms two principal geochemical associations: the Pb-Ag group, representing the galena-dominated mineralization, and the Zn-Cd-Sb group, characteristic of the sphalerite-bearing zones. This relationship confirms the interpretation of a hydrothermal origin of mineralization with subsequent geochemical differentiation during ore formation.

To further examine the spatial variation of the analyzed elements, a geochemical contour analysis was performed for Horizon IX (Fig. 6). This level represents the continuation of mineralization zones identified in Horizon VIII, allowing for comparison of compositional patterns and element associations between successive ore bodies.

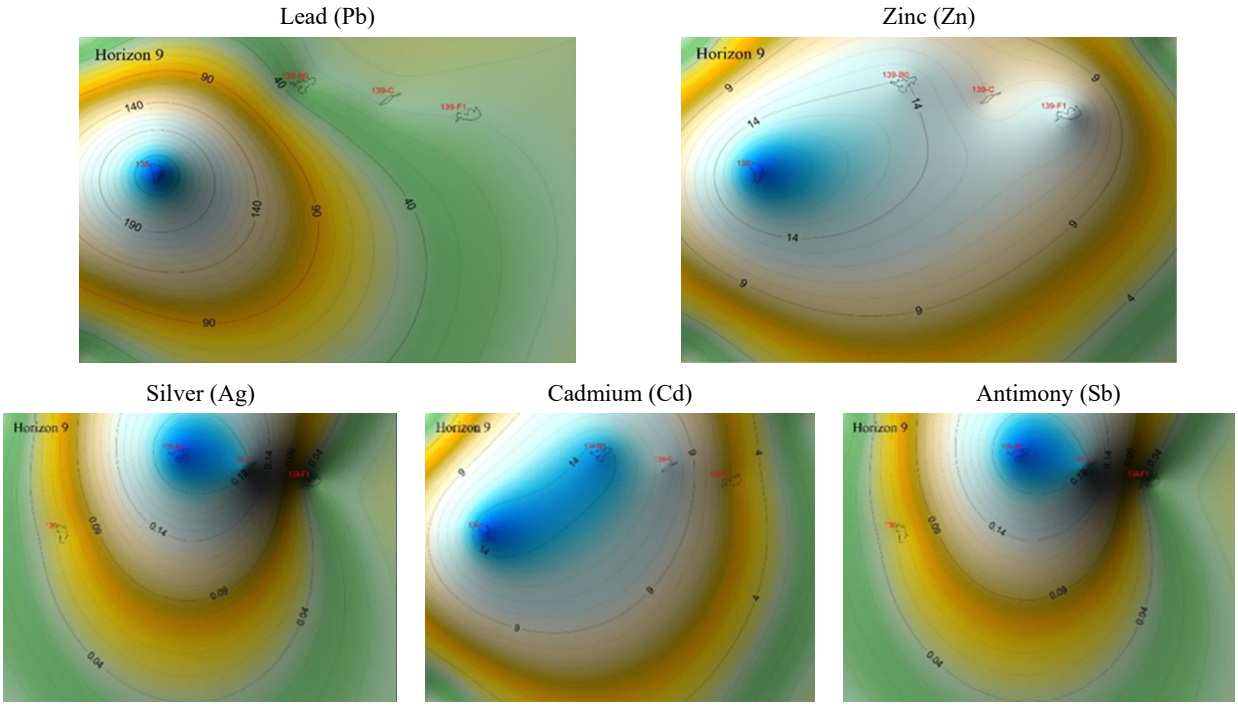

Figure 6. Spatial distribution maps of selected elements in Horizon IX

The obtained maps reveal that, similar to Horizon VIII, Horizon IX exhibits a well-defined Pb-Zn zoning pattern. Lead (Fig. 6a) is most concentrated in the central portion of the ore body, forming the core of mineralization. Zinc (Fig. 6b) occurs more uniformly throughout the ore zone but dominates in the peripheral sectors, typical of sphalerite (ZnS) mineralization. Silver (Fig. 6c) spatially coincides with the Pb-enriched zones, indicating a paragenetic relationship with galena (PbS) and Ag-bearing phases. Cadmium (Fig. 6d) shows enrichment around the Zn-rich margins, suggesting isomorphic substitution of Cd within the sphalerite lattice. Antimony (Fig. 6e) displays a broader and more dispersed distribution compared to Ag and Cd. Its elevated concentrations in both central and marginal parts confirm a dual geochemical association, occurring together with both Pb- and Zn-bearing minerals. Overall, Horizon IX reflects a repetition of the paragenetic trend observed in Horizon VIII: a clearly defined Pb-Ag core surrounded by Zn-Cd-Sb halos, illustrating the vertical continuity of hydrothermal processes and zonal mineralization within the Trepça deposit.

The next level of investigation focuses on Horizon X, where the spatial relationship among Pb, Zn, Ag, Cd, and Sb continues to illustrate the vertical evolution of hydrothermal mineralization within the Trepça system (Fig. 7).

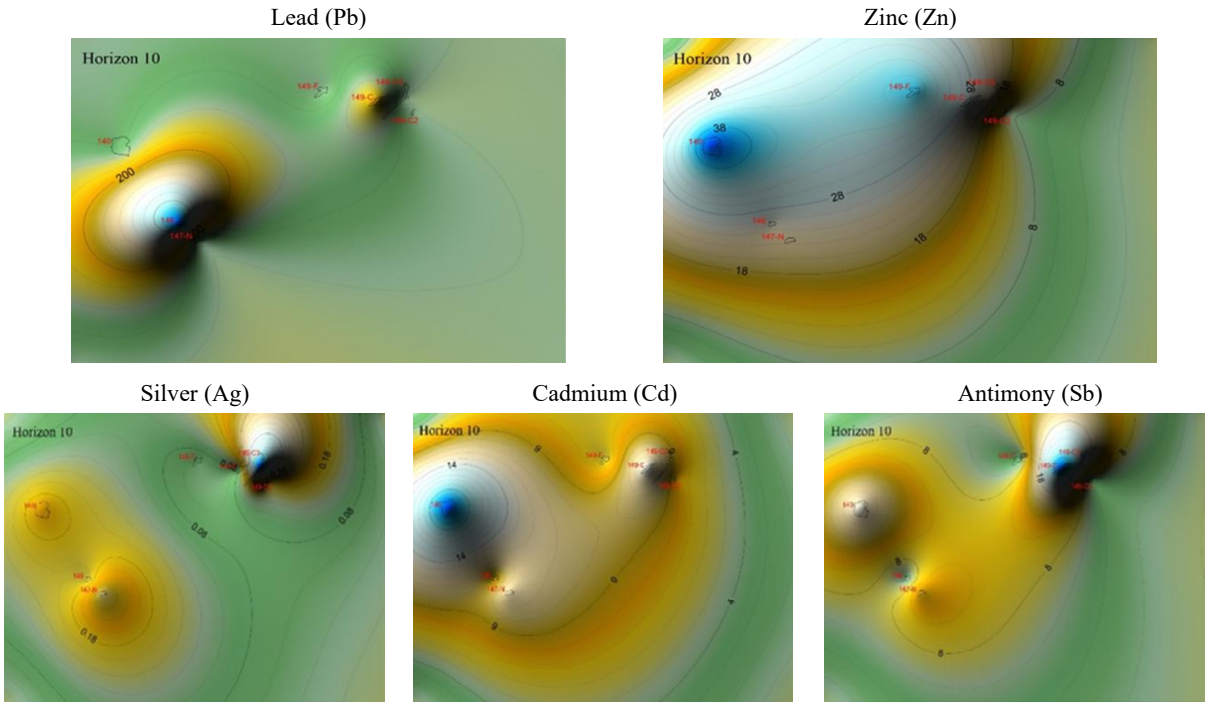

Figure 7. Spatial distribution maps of selected elements in Horizon X

The obtained results show a clear zoning distribution pattern, where Pb and Zn form the main mineralization core. Lead (Fig. 7a) dominates the central parts of the ore bodies, while zinc (Fig. 7b) is distributed in surrounding zones, reflecting the typical paragenetic arrangement of galena (PbS) and sphalerite (ZnS). Silver (Fig. 7c) exhibits a strong spatial association with Pb, confirming its occurrence within galena and Ag-bearing sulfides. Cadmium (Fig. 7d) appears primarily in Zn-enriched zones, reflecting isomorphic substitution within sphalerite lattices, similar to the trends observed in the previous horizons. However, antimony (Fig. 7e) displays a distinctive behavior in Horizon X: its distribution is more closely linked to both Ag- and Pb-rich areas, suggesting a later-stage remobilization and association with Ag-bearing minerals such as tetrahedrite or boulangerite. Thus, Horizon X reflects an intensified paragenetic relationship between Ag and Sb in addition to the established Pb-Zn-Cd zonation, indicating a more complex hydrothermal evolution and possible secondary enrichment at later mineralization stages.

The final analyzed level, Horizon XI, represents the deepest examined section within the studied system and provides insight into the vertical continuity of Pb-Zn-Ag-Cd-Sb mineralization (Fig. 8). By comparing this horizon with the upper ones, it becomes possible to identify geochemical trends along the ore-bearing structure and determine whether zoning persists in deeper mineralization zones.

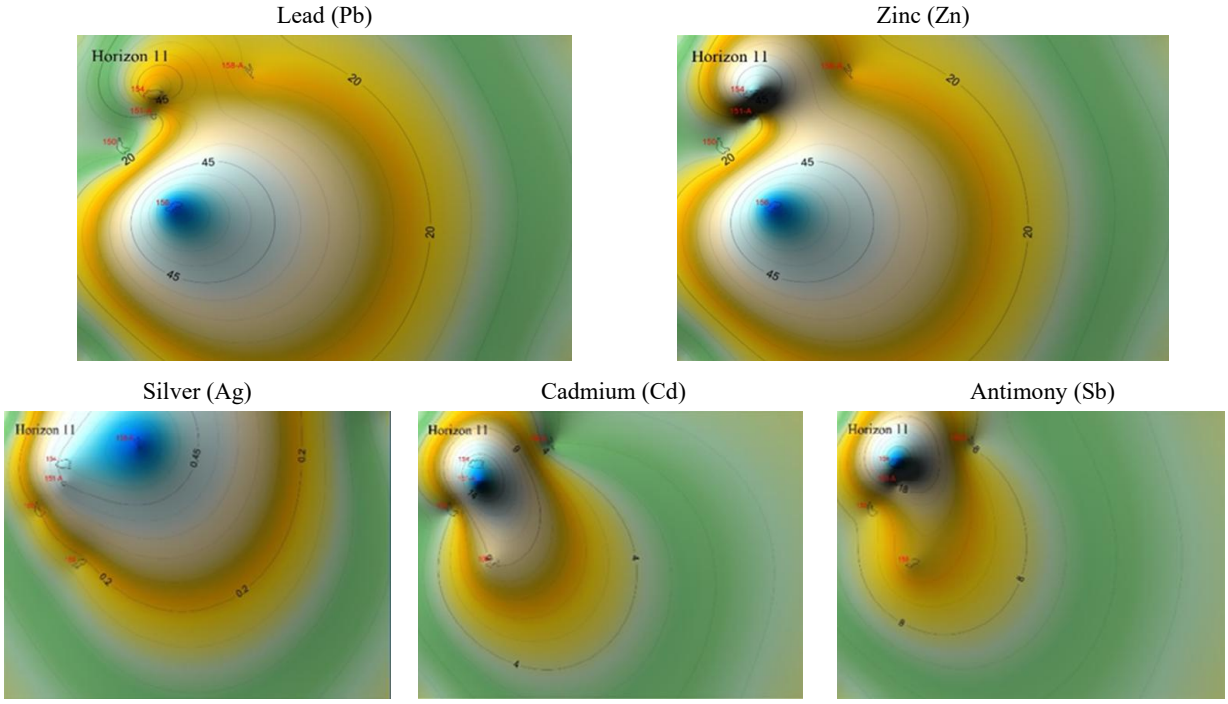

Figure 8. Spatial distribution maps of selected elements in Horizon XI

Horizon XI, similar to the upper levels, exhibits a well-defined Pb-Zn zonation; however, the geochemical patterns suggest enhanced enrichment in Ag and Cd within the sphalerite-bearing zones. Lead (Fig. 8a) remains concentrated in the core of the ore body, while zinc (Fig. 8b) occurs peripherally, forming typical galena-sphalerite zoning. Silver (Fig. 8c) reaches its maximum concentrations in this horizon, showing strong spatial correlation with both Pb and Zn mineralization, which implies simultaneous deposition of Ag-bearing phases at later hydrothermal stages.

Cadmium (Fig. 8d) also presents high values in several ore bodies, largely associated with Zn-rich areas, confirming its isomorphic substitution within sphalerite lattices. Antimony (Fig. 8e) demonstrates a broader spatial distribution than in the upper horizons, overlapping both Zn- and Ag-enriched regions. This indicates its intermediate geochemical affinity, possibly linked to the presence of late-stage minerals such as tetrahedrite or boulangerite.

The spatial distribution observed in Horizon XI confirms the vertical persistence of Pb-Zn-Ag-Cd-Sb zonation within the Trepça ore system, with increasing Ag and Cd contents at depth, reflecting the thermal and compositional evolution of hydrothermal fluids responsible for the ore formation.

4.3. General interpretation of Pb-Zn-Ag-Cd-Sb distribution across Horizons VIII-XI

The comparative spatial analysis of Horizons VIII to XI within the Trepça ore system reveals a coherent vertical zonation pattern that reflects both the geochemical evolution and paragenetic relationships among the studied elements. In all examined levels, lead and zinc maintain a dual-core structure characteristic of polymetallic sulfide deposits: galena-rich centers surrounded by sphalerite-bearing halos. This structural continuity indicates the persistence of the hydrothermal flow regime and metal precipitation fronts during successive stages of mineralization. Silver is consistently associated with lead, displaying a strong paragenetic affinity with galena, but its concentration gradually increases with depth from Horizon VIII down to Horizon XI, suggesting a late-stage remobilization of Ag-bearing phases under more reducing and thermally stable conditions.

Cadmium follows zinc throughout all horizons, confirming its incorporation by isomorphic substitution within the sphalerite lattice. Its downward enrichment trend also confirms the interpretation of progressive metal differentiation in response to evolving temperature and fluid chemistry. Antimony shows the most dynamic spatial behavior: in the upper

horizons, it is more closely related to zinc mineralization, whereas in deeper levels (particularly Horizons X and XI), it increasingly overlaps with both Pb and Ag distributions. This indicates a change in redox and sulfur fugacity conditions that favored the precipitation of Sb-bearing sulfosalts such as tetrahedrite and boulangerite.

Taken together, the four horizons demonstrate that the Trepça mineralization system preserves a vertically continuous Pb-Zn-Ag-Cd-Sb zoning. The upper levels are dominated by the classical Pb-Zn paragenesis, while deeper sections reveal stronger Ag and Cd enrichment and a progressive geochemical convergence of Sb with Pb- and Ag-bearing minerals. Such a pattern is typical of hydrothermal replacement systems affected by fluid evolution, temperature gradients, and secondary remobilization. Therefore, the vertical geochemical coherence observed across Horizons VIII-XI provides clear evidence of a unified hydrothermal process that governed metal transport and deposition within the Trepça ore field.

4. Conclusions

The geochemical and spatial analysis of Horizons VIII-XI within the Trepça ore field demonstrates a vertically continuous polymetallic zonation that is characteristic of hydrothermal Pb-Zn systems. Across all studied levels, the mineralization is marked by a well-defined Pb-Ag core surrounded by Zn-Cd-Sb halos, reflecting a consistent hydrothermal regime and gradual differentiation of metal-bearing fluids during successive stages of ore formation. The correlation and mapping results confirm that lead and silver form a stable paragenetic association, whereas zinc hosts cadmium through isomorphic substitution within sphalerite. This spatial regularity confirms the interpretation of a unified and long-lived hydrothermal process responsible for the polymetallic mineralization of Trepça.

The vertical trends reveal an evolution of geochemical conditions with increasing depth. Silver enrichment in Horizons X and XI indicates its remobilization and redeposition at later hydrothermal stages under more reducing conditions, while cadmium consistently follows zinc, suggesting progressive temperature and fluid composition changes during downward mineral deposition. Antimony shows the most variable pattern, being closely related to zinc in upper horizons, but increasingly associated with lead and silver at depth. This transition implies a shift in redox potential and sulfur fugacity, favouring the formation of Sb-bearing sulfosalts such as tetrahedrite and boulangerite during the final mineralization phases.

These findings highlight the genetic and economic significance of critical elements within the Trepça ore system. The identified Pb-Ag and Zn-Cd-Sb geochemical assemblages provide reliable indicators for exploration, mine planning, and potential by-product recovery strategies. The established workflow, combining systematic sampling, ICP-MS analysis and spatial-statistical modeling, provides a robust methodological basis for assessing the distribution of critical and valuable trace elements in mature polymetallic deposits, contributing to both geological interpretation and sustainable resource utilization in the Trepça district.

Author contributions

Conceptualization: FK; Data curation: FK; Formal analysis: FK, BS; Investigation: FK, BS; Methodology: FK; Software: BS; Supervision: BS; Validation: FK; Visualization: FK, BS; Writing – original draft: FK; Writing – review & editing: FK, BS. All authors have read and agreed to the published version of the manuscript.

Funding

This research received no external funding.

Acknowledgements

The authors would like to express their gratitude to the journal editor and reviewers for their valuable comments and suggestions.

Conflicts of interest

The authors declare no conflict of interest.

Data availability statement

The original contributions presented in the study are included in the article, further inquiries can be directed to the corresponding author.

References

[1] Hyseni, S., Durmishaj, B., Fetahaj, B., & Large, D. (2010). Trepça ore belt and lead and zinc distribution in Badovc mineral deposit, Kosovo (SE Europe). *Journal of Engineering and Applied Sciences*, *5*(8), 1-9.

[2] Gashi, F., Bilinski, S.F., Bilinski, H., Thaçi, B., & Shosholli, S. (2017). Chemical determination of heavy metals in Pb and Zn concentrates of Trepça (Kosovo) and correlations coefficients study between chemical data. *Rudarsko-Geološko-Naftni Zbornik*, *32*(2), 29-35. https://doi.org/10.17794/rgn.2017.2.4

[3] Haziri, M. (2018). The first investigations of Britains in Trepça's Mine in Stan Terg. *Acta Universitatis Danubius. Relationes Internationales*, *11*(2), 219-225.

[4] Ilijanić, N., Miko, S., Petrinec, B., & Franić, Z. (2014). Metal deposition in deep sediments from the Central and South Adriatic Sea. *Geologia Croatica*, *67*(3), 185-205. https://doi.org/10.4154/gc.2014.14

[5] Novak, A., Verbovšek, T., & Popit, T. (2017). Heterogeneously composed Lozice fossil landslide in Rebrnice area, Vipava Valley. *Geologija*, *60*(1), 145-155. https://doi.org/10.5474/geologija.2017.011

[6] Hetemi, M., & Kastrati, S. (2008). Lead-zinc resources in Kosovo. *Mining Magazine*, 1-10.

[7] Galán, E., Romero-Baena, A.J., Aparicio, P., & González, I. (2019). A methodological approach for the evaluation of soil pollution by potentially toxic trace elements. *Journal of Geochemical Exploration*, *203*, 96-107. https://doi.org/10.1016/j.gexplo.2019.04.005

[8] Amralinova, B. (2023). Rare-metal mineralization in salt lakes and the linkage with composition of granites: Evidence from Burabay Rock Mass (Eastern Kazakhstan). *Water*, *15*(7), 1386. https://doi.org/10.3390/w15071386

[9] Dyachkov, B.A., Amralinova, B.B., Mataybaeva, I.E., Dolgopolova, A.V., Mizerny, A.I., & Miroshnikova, A.P. (2017). Laws of formation and criteria for predicting nickel content in weathering crusts of east Kazakhstan. *Journal of the Geological Society of India*, *89*(5), 605-609. https://doi.org/10.1007/s12594-017-0650-7

[10] Šajn, R., Ristović, I., & Čeplak, B. (2022). Mining and metallurgical waste as potential secondary sources of metals: A case study for the west Balkan region. *Minerals*, *12*(5), 547. https://doi.org/10.3390/min12050547

[11] ICMM. (2006). *Minerals map of Kosovo*.

[12] Neves, O., Moreno, F., Pinheiro, D., Pinto, M.C., & Inácio, M. (2024). Soil low-density geochemical mapping of technology-critical elements (TCEs) and its environmental implications: The case of lithium in Portugal. *Science of The Total Environment*, *934*, 173207. https://doi.org/10.1016/j.scitotenv.2024.173207

[13] Sedda, L., De Giudici, G., Fancello, D., Podda, F., & Naitza, S. (2023). Unlocking strategic and critical raw materials: Assessment of zinc and REEs enrichment in tailings and Zn-carbonate in a historical mining area (Montevecchio, SW Sardinia). *Minerals*, *14*(1), 3. https://doi.org/10.3390/min14010003

[14] Dang, D.H., Kim, J., Lee, J., & Kim, S. (2021). Critical raw materials for the EU: Historical evolution, current status, and future perspectives. *Resources Policy*, *74*, 102274. https://doi.org/10.1016/j.resourpol.2021.102274

[15] European Commission. (2023). *Critical Raw Materials Act and the 2023 list of critical raw materials and strategic raw materials.* Brussels: Publications Office of the European Union. https://doi.org/10.2873/724890
[16] Sverdrup, H.U., van Allen, O., & Haraldsson, H.V. (2024). Assessing aspects of cadmium supply, recycling and environmental pollution with respect to future photovoltaic technology demands and environmental policy goals. *Water, Air, & Soil Pollution*, *235*(4), 247. https://doi.org/10.1007/s11270-024-07027-2
[17] Blumbergs, E., Serga, V., Platacis, E., Maiorov, M., & Shishkin, A. (2021). Cadmium recovery from spent Ni-Cd batteries: A brief review. *Metals*, *11*(11), 1714. https://doi.org/10.3390/met11111714
[18] Anderson, C.G. (2019). Antimony production and commodities. *SME Mineral Processing & Extractive Metallurgy Handbook*, *2*, 1557-1568.
[19] Dembele, S., Akcil, A., & Panda, S. (2022). Technological trends, emerging applications and metallurgical strategies in antimony recovery from stibnite. *Minerals Engineering*, *175*, 107304. https://doi.org/10.1016/j.mineng.2021.107304
[20] Avdullahi, S. (2002). *Hidrogjeologjia e fushës xeherore "Trepça"*. Tiranë: Universiteti i Tiranës.
[21] Boente, C., Baragaño, D., García-González, N., Forján, R., Colina, A., & Gallego, J.R. (2022). A holistic methodology to study geochemical and geomorphological control of the distribution of potentially toxic elements in soil. *Catena*, *208*, 105730. https://doi.org/10.1016/j.catena.2021.105730
[22] Nazirova, A., Kalimoldayev, M., Abdoldina, F., & Dubovenko, Y. (2022). Optimization of an information system module for solving a direct gravimetry problem using a genetic algorithm. *Eastern-European Journal of Enterprise Technologies*, *2*(9(116)), 21-34. https://doi.org/10.15587/1729-4061.2022.253976
[23] Balaram, V., & Satyanarayanan, M. (2022). Data quality in geochemical elemental and isotopic analysis. *Minerals*, *12*(8), 999. https://doi.org/10.3390/min12080999
[24] Zaresefat, M., Derakhshani, R., & Griffioen, J. (2024). Empirical Bayesian Kriging, a robust method for spatial data interpolation of a large groundwater quality dataset from the Western Netherlands. *Water*, *16*(18), 2581. https://doi.org/10.3390/w16182581
[25] Umarbekova, Z.T., Zholtayev, G.Z., Zholtayev, G.Z., Amralinova, B.B., & Mataibaeva, I.E. (2020). Silver halides in the hypergene zone of the Arkharly gold deposit as indicators of their formation in dry and hot climate. *International Journal of Engineering Research and Technology*, *13*(1), 181-190. https://doi.org/10.37624/ijert/13.1.2020.181-190
[26] Daya, A.A., & Bejari, H. (2015). A comparative study between simple kriging and ordinary kriging for estimating and modeling the Cu concentration in Chehlkureh deposit, SE Iran. *Arabian journal of Geosciences*, *8*(8), 6003-6020. https://doi.org/10.1007/s12517-014-1618-1
[27] Spadoni, M., Cavarretta, G., & Patera, A. (2004). Cartographic techniques for mapping the geochemical data of stream sediments: The "sample catchment basin" approach. *Environmental Geology*, *45*(5), 593-599. https://doi.org/10.1007/s00254-003-0926-7
[28] Balaram, V., & Subramanyam, K.S.V. (2022). Sample preparation for geochemical analysis: Strategies and significance. *Advances in Sample Preparation*, *1*, 100010. https://doi.org/10.1016/j.sampre.2022.100010
[29] Nelson, F. (2014). *Quality control program for a geochemical laboratory*. Doctoral dissertation. Saskatchewan, Canada: Department of Geological Sciences, University of Saskatchewan.
[30] Smee, B.W., Bloom, L., Arne, D., & Heberlein, D. (2024). Practical applications of quality assurance and quality control in mineral exploration, resource estimation and mining programmes: A review of recommended international practices. *Geochemistry: Exploration, Environment, Analysis*, *24*(2), 45-63. https://doi.org/10.1144/geochem2023-046
[31] Shahrestani, S., Sanislav, I., & Fereydooni, H. (2025). Rotation-based outlier detection for geochemical anomaly identification in stream sediment multivariate data. *Earth Science Informatics*, *18*(3), 1-18. https://doi.org/10.1007/s12145-025-01811-2
[32] Dubovenko, Y.I., Nazirova, A.B., & Abdoldina, F.N. (2022). Data-driven preprocessing of gravity data in oilfield GIS monitoring system in Kazakhstan. *International Conference Monitoring of Geological Processes and Ecological Condition of the Environment*, *1*, 1-4. https://doi.org/10.3997/2214-4609.2022580267
[33] Geboy, N.J., & Engle, M.A. (2011). *Quality assurance and quality control of geochemical data: A primer for the research scientist*. US Department of the Interior, US Geological Survey.

Геохімічний розподіл і кореляції Cd-Ag-Sb щодо Pb-Zn мінералізації в родовищі Трепча, Косово

Ф. Кутловці, Б. Сінані

Мета. Вивчення геохімічного розподілу та міжелементних кореляцій кадмію (Cd), срібла (Ag) і сурми (Sb) у поліметалічній рудній системі свинець-цинк (Pb-Zn) родовища Трепча (Косово) для встановлення їхніх парагенетичних зв'язків з основними сульфідними мінералами – галенітом і сфалеритом, та визначення просторових закономірностей розподілу у межах рудних зон.

Методика. Репрезентативні проби відібрано з кожного активного рудного тіла горизонтів VIII-XI родовища Трепча. Кожну пробу висушували, подрібнювали у декілька стадій, піддавали кислотному розкладанню та аналізували методом індуктивно зв'язаної плазми з мас-спектрометрією (ICP-MS). Отримані аналітичні дані були статистично оброблені з визначенням описових параметрів та коефіцієнтів кореляції Пірсона. Просторовий розподіл елементів візуалізовано за допомогою програмного забезпечення Surfer з побудовою геохімічних карт.

Результати. Визначено вміст кадмію, що становить від 34 до 1125 ppm (середнє ≈ 308 ppm), срібла – від 20 до 389 ppm (середнє ≈ 93 ppm), сурми – від 42 до 512 ppm (середнє ≈ 171 ppm). Встановлено тісний позитивний зв'язок між Ag і Pb ($r = 0.94$) та між Cd і Zn ($r = 0.77$), що свідчить про існування двох домінуючих геохімічних асоціацій: Pb-Ag парагенетичної групи та Zn-Cd-Sb асоціації. Вертикальний і просторовий розподіл елементів підтверджує безперервну Pb-Zn-Ag-Cd-Sb зональність, характерну для гідротермальних систем заміщення.

Наукова новизна. Представлене дослідження вперше подає інтегровану статистичну та просторову характеристику розподілу елементів Ag-Cd-Sb щодо Pb-Zn мінералізації в родовищі Трепча. Показано вертикальну спадкоємність геохімічних закономірностей і еволюцію умов гідротермальних процесів, що контролювали формування рудної системи.

Практична значимість. Представлене дослідження вперше подає інтегровану статистичну та просторову характеристику розподілу елементів Ag-Cd-Sb щодо Pb-Zn мінералізації в родовищі Трепча. Показано вертикальну спадкоємність геохімічних закономірностей та еволюцію умов гідротермальних процесів, що контролювали формування рудної системи.

Ключові слова: *Трепча, родовище, геохімія, розподіл, критичні елементи*

Publisher's note

All claims expressed in this manuscript are solely those of the authors and do not necessarily represent those of their affiliated organizations, or those of the publisher, the editors and the reviewers.